Turkish Journal of Electrical Engineering & Computer Sciences

http://journals.tubitak.gov.tr/elektrik/

Research Article

Turk J Elec Eng & Comp Sci
(2020) 28: 3126 – 3136

doi:10.3906/elk-1911-104

# Design of a miniaturized planar microstrip Wilkinson power divider with harmonic cancellation

**Saeedeh LOTFI, Saeed ROSHANI*, Sobhan ROSHANI**
Department of Electrical Engineering, Kermanshah Branch, Islamic Azad University, Kermanshah, Iran

**Received:** 15.11.2019 • **Accepted/Published Online:** 29.05.2020 • **Final Version:** 30.11.2020

**Abstract:** In this paper, a compact microstrip Wilkinson power divider is designed and proposed using rectangular-shaped resonator cells. The presented resonator cells are used instead of quarter-wave length branches in the traditional structure to reduce the circuit size, increase the bandwidth, and eliminate the unwanted harmonics. The designed resonator behavior is studied analytically and the locations of transmission zeros are investigated using transfer function and LC equivalent circuit methods. The proposed power divider (PD) operates at 2 GHz frequency and suppresses the 2nd to 14th unwanted harmonics. The proposed PD achieves approximately 50% size reduction and 40% fractional bandwidth (FBW). The abilities of desirable size reduction and harmonic suppression along with simple structure and wide FBW make the proposed divider a good choice for the modern communication systems, such as multistage power amplifier applications. The proposed divider is implemented and measured. The measurement results verify the simulation responses.

**Key words:** Microstrip, Wilkinson power divider, LC equivalent model, transmission zero

## 1. Introduction

The first Wilkinson power divider (WPD) was introduced in 1960 by J. Wilkinson [1]. The Wilkinson divider is a three-port passive element, which divides input power with an equal or unequal division ratio [2]. Emerging RF/microwave communications has led to the design and production of high frequency devices with features, such as high performance, compact size, low cost, and light weight [3]. Compact size and harmonic canceling are known as advantages in PD design. In terms of size reduction and harmonic suppression, comprehensive studies have been done in recent years [4–22]. In [3], a compact microstrip Bagley divider is introduced, using dual transmission lines technique. A small divider with a wideband response and unequal planar design is presented in [4], which includes nonuniform microstrip lines and two asymmetric coupled transmission line sections. Applying an electromagnetic bandgap (EBG) in power divider structure can provide a compact PD with harmonic suppression [5]. Using microstrip resonators instead of 70.7 Ω transmission lines in conventional divider structure leads to a decrease in the size and eliminates the harmonics in [6–11]. In [12] open stubs are applied to eliminate 2nd and 3rd harmonics in Gysel divider design, but size reduction and harmonic rejection in this work are not superior. In [13], two varactor capacitors are used in WPD to make tunable transmission-line transformers and in [14] capacitors are used to create composite transmission lines for size reduction aims. Unfortunately using lumped reactive components are not desirable in high-frequency microwave design.

*Correspondence: s_roshany@yahoo.com

Two 4-way dividers are presented in [15, 16]. The divider in [15] has a bandpass filtering response, which utilizes frequency-dependent coupling structures. The presented divider in [16] suffers from large size and existence of the unwanted harmonics in frequency response. In [17], a simple PD with two tunable transmission zeros is presented using cascaded inhomogeneous coupled-lines. In [18], stub loaded lines are applied instead of two traditional $\lambda/4$ branches, to decrease the circuit size and achieve better harmonic elimination in the GSM frequency band. In [19], a microstrip Wilkinson PD with harmonic suppression is designed, using resonator cells. In this reported work, lowpass filters are used instead of $\lambda/4$ transmission lines. In some dividers lumped reactive components are used to decrease the circuit area and eliminate unwanted harmonics [20], but this method is undesirable in the fabrication process [21].

Also, a neuro-based approach to designing a Wilkinson power divider is published in [22], which is composed of two lowpass filters instead of two quarter wavelength line in conventional circuit. Applying microstrip resonators is useful in designing good performance RF circuits as in [23–26]. Another Wilkinson power divider with harmonic suppression and bandpass filtering response is suggested in [27], which used open and short stubs and even-odd mode analyses, but this design has a large circuit size.

In this paper, a WPD using resonators is presented. The applied main resonator is formed by rectangular-shaped and modified T-shaped resonators. The main resonator is replaced instead of quarter-wavelength branches in conventional circuit. The main resonator can reduce the circuit area and reject the higher order of harmonics. The proposed PD can correctly work from 1.60 GHz to 2.40 GHz, which shows 40% fractional bandwidth. Also, the proposed PD has an acceptable level of output ports isolation better than 22 dB. In order to investigate the proposed Wilkinson PD behavior, its LC equivalent model is calculated and its transfer function is extracted.

## 2. Wilkinson power divider design

Figure 1 shows the traditional WPD including two $\lambda/4$ transmission lines and a $2Z_0$ lumped resistor [2]. In the proposed divider, two $\lambda/4$ transmission lines are replaced by two main resonator cells for harmonic suppression and size reduction. The design procedure is explained in the next section.

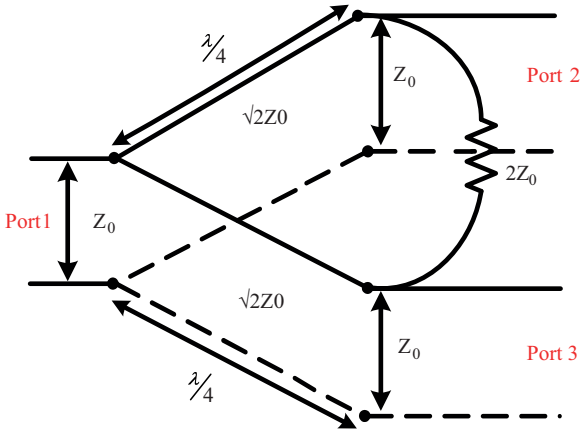


**Figure 1**. Conventional Wilkinson PD.

## 3. Main resonator design

The proposed main resonator cell is depicted in Figure 2. The main resonator is made of a modified T-shaped resonator and four rectangular-shaped resonators.

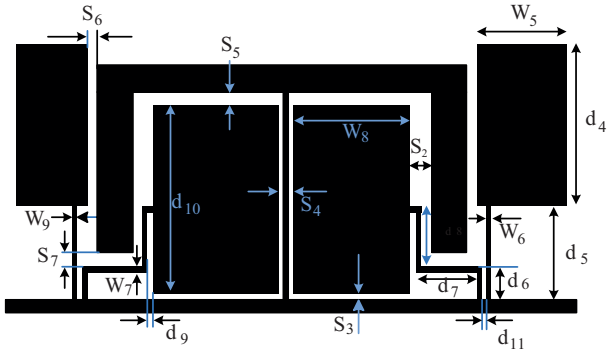


**Figure 2**. Proposed main resonator.

Figure 3a depicts the modified T-shaped resonator. To analyze the modified T-shaped resonator, its LC equivalent model is obtained. The proposed LC equivalent model of the modified T-shaped resonator is given in Figure 3b. The electromagnetic (EM) simulation results of the modified T-shaped resonator and LC equivalent model simulation, which are in good agreement, are illustrated in Figure 3c.

The modified T-shaped resonator has a transmission zero (Tz1) at 4.20 GHz, which is located near the second harmonic as depicted in Figure 3c. The created transmission zero has 47 dB attenuation level, which can suppress the second harmonic in the stopband.

The dimensions of the modified T-shaped resonator are as follows: d1 = 7.7, d2 = 2.4, d3 = 6.3, W1 = 0.4, W2 = 0.7, W3 = 0.1, W4 = 0.2, S1 = 0.7 (all in millimeter). The obtained values for the LC equivalent model of the presented modified T-shaped resonator are listed in Table 1.

**Table 1**. Computed values for LC equivalent model of the modified T-shaped resonator (Units: C, pF; L, nH).

| Parameters | L'1 | L2 | L3 | L4 |
|---|---|---|---|---|
| Calculated | 4.23 | 2.50 | 2.09 | 1.05 |
| Parameters | C'1 | C2 | C3 | C4 |
| Calculated | 0.19 | 0.15 | 0.11 | 0.05 |

Inductance and capacitance values are computed using open-ended lines and high impedance lines equations. Formulas for these lossless lines are given in (1) and (2) [2].

$$L_S = \frac{1}{w} \times Z_S \times \sin\left(\frac{2\pi l}{\lambda_g}\right) \tag{1}$$

$$C_S = \frac{1}{w} \times \frac{1}{Z_S} \times \tan\left(\frac{\pi l}{\lambda_g}\right) \tag{2}$$

where $Z_S$ is the characteristic impedance of the line and $\lambda_g$ denotes the guided wavelength. Locations of the transmission zeros are obtained using transfer function (TF). The transmission zeros are computed using

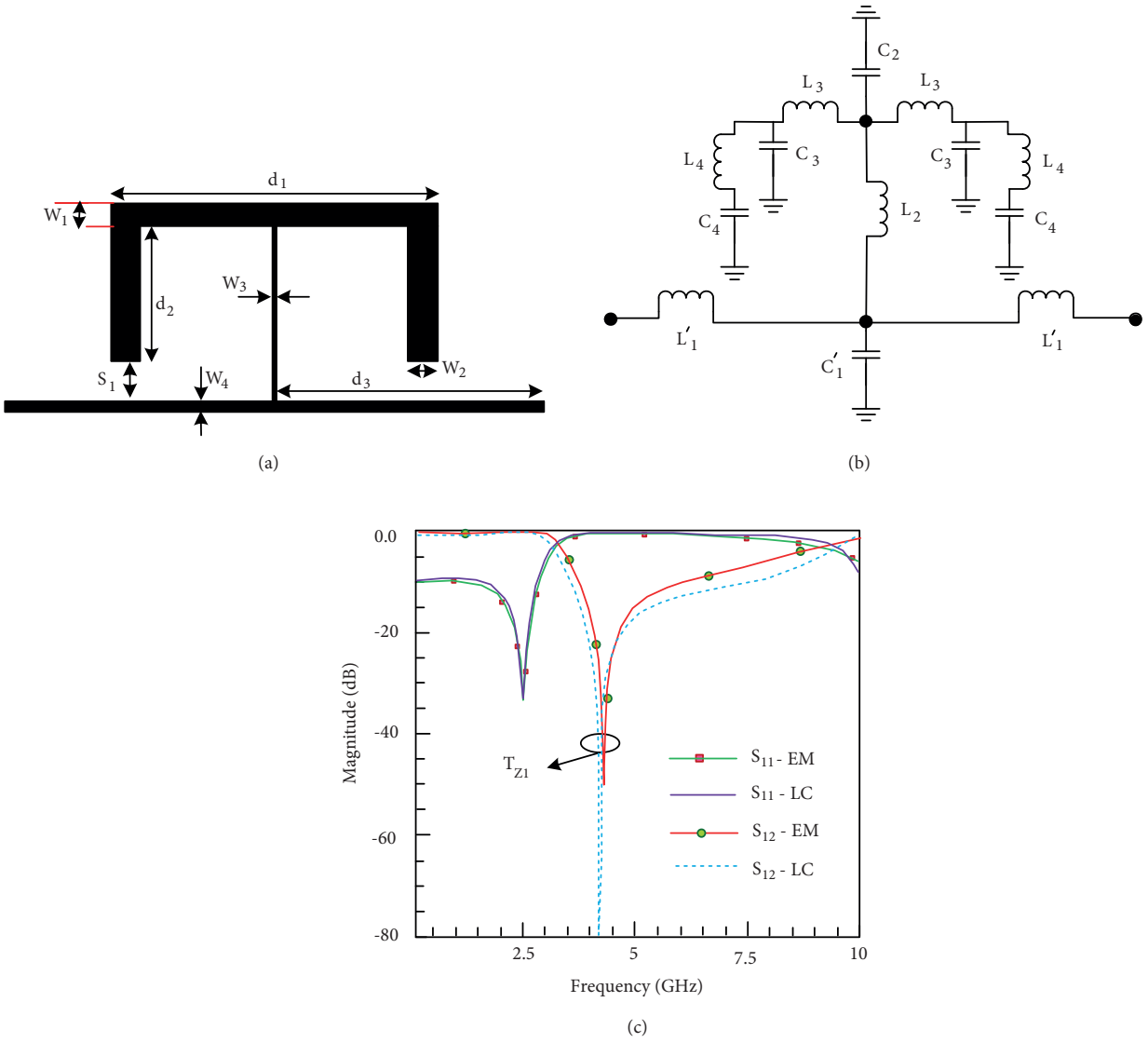


**Figure 3**. Proposed modified T-shaped resonator, (a) layout, (b) proposed LC equivalent model, (c) EM simulation and circuit simulation results.

the numerator of the TF. The TF is extracted from Figure 3b, which is written in (3).

$$\frac{V_o}{V_i}|_{T-Shaped} = \frac{r \times X}{(r + L_1 S)(r + L_1 S + 2X)} \tag{3}$$

where "r = 50Ω", "X" and "A" parameters are defined in (4) and (5), respectively as follows:

$$X = \frac{A + 2L_2 S + AC_2 L_2 S^2}{2 + AC_1 S + AC_2 S + 2C_1 L_2 S^2 + AC_1 C_2 L_2 S^3} \tag{4}$$

$$A = \frac{1 + C_3 L_3 S^2 + C_4 L_3 S^2 + C_4 L_4 S^2 + C_3 C_4 L_3 L_4 S^4}{s(C_3 + C_4 + C_3 C_4 L_4 S^2)} \tag{5}$$

If the numerator of the TF is equated to zero, the location of the transmission zero (TZ) will be defined, as demonstrated in (6). According to this equation, the location of the TZ can be controlled by changing the values of the inductances and capacitances. In the other words, by changing the values of the inductances and capacitances, the parameters of P1, P2, P3, b, and c will be changed; therefore, the TZ location can be justified.

$$T_{z1} = \frac{1}{2\pi}\sqrt{|(-\frac{b}{3c}) - (P_1) + (P_2) + (P_3)|} \tag{6}$$

where "$P_1$","$P_2$", and "$P_3$" are defined in (7), (8), and (9) as follows:

$$P_1 = \frac{\sqrt[3]{2}a}{(-2b^3 + 9abc - 27c^2 + \sqrt{4(-b^2+3ac)^3 + (-2b^3+9abc-27c^2)^2})^{\frac{1}{3}}} \tag{7}$$

$$P_2 = \frac{\sqrt[3]{2}b^2}{3c(-2b^3 + 9abc - 27c^2 + \sqrt{4(-b^2+3ac)^3 + (-2b^3+9abc-27c^2)^2})^{\frac{1}{3}}} \tag{8}$$

$$P_3 = \frac{(-2b^3 + 9abc - 27c^2 + \sqrt{4(-b^2+3ac)^3 + (-2b^3+9abc-27c^2)^2})^{\frac{1}{3}}}{\sqrt[3]{32}c} \tag{9}$$

where "$a$", "$b$", and "$c$" parameters can be obtained in (10), (11), and (12) respectively as bellow:

$$a = (C_4(2L_2 + L_3 + L_4) + C_3(2L_2 + L_3) + C_2L_2) \tag{10}$$

$$b = C_3C_4L_4(2L_2 + L_3) + C_2L_2(C_3L_3 + C_4(L_3 + L_4)) \tag{11}$$

$$c = C_2L_2C_3C_4L_3L_4 \tag{12}$$

The proposed modified T-shaped resonator did not have a good suppression level in the stopband. In order to have an acceptable harmonic suppression, more transmission zeros should be added in the stopband. Thus, four rectangular-shaped resonator cells are added to the modified T-shaped resonator. The rectangular shaped resonators help to create better stopband. The LC equivalent model for the main resonator, which is depicted in Figure 2, and its frequency response are illustrated in Figures 4a and 4b, respectively.

As seen in Figure 4b, the proposed structure can create two transmission zeros at 3.58 GHz and 4.75 GHz. These transmission zeros can suppress more harmonics in WPD design. The presented main resonator dimensions are as follows: d4 = 2.4, d5 = 1.4, d6 = 0.5, d7 = 1.2, d8 = 0.9, d9 = 0.1, d10 = 2.8, d11 = 0.11, W3 = 0.1, W5 = 2.1, W6 = 0.1, W7 = 0.1, W8 = 2.6, S3 = 0.1, S4 = 0.3, S5 = 0.2, S6 = 0.2, S7 = 0.2 (all in millimeter). The computed values for the LC equivalent model of the proposed main resonator are listed in Table 2.

The TF of the designed main resonator is computed in (13).

$$\frac{V_o}{V_i}|_{mainresonator} = \frac{(CF^2r)}{((L_1S(r+L_{10}S) + F(r+(L_1+L_{10})S))(L_1S(r+L_{10}S) + 2C(F+r+L_{10}S) + F(r+(L_1+L_{10})S)))} \tag{13}$$

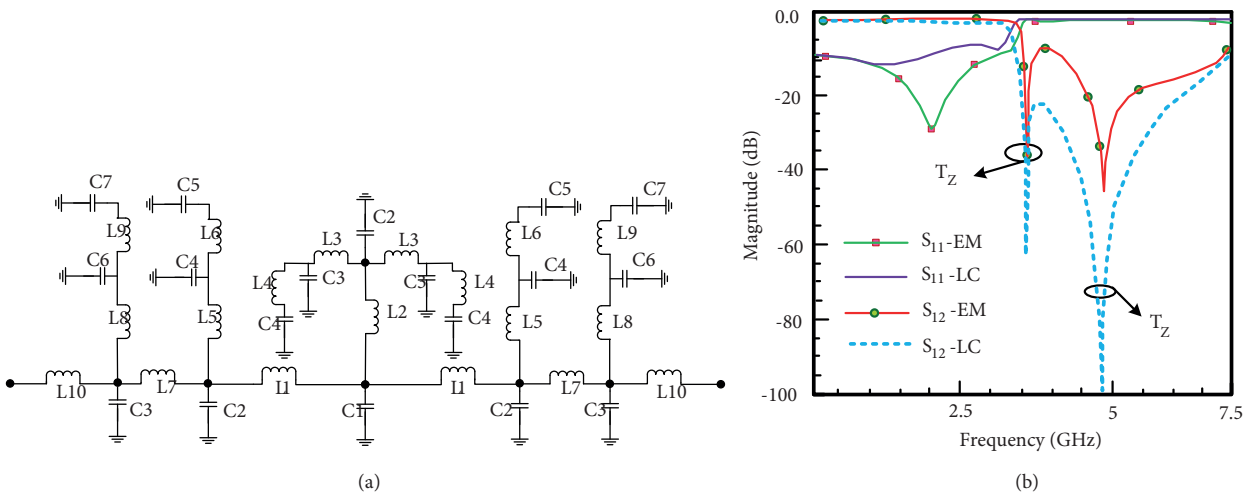


**Figure 4**. Proposed main resonator, a) LC equivalent model, b). EM and LC simulation results.

**Table 2**. Computed values for LC equivalent model of proposed main resonator (Units: C, pF; L, nH).

| Parameters | L1 | L2 | L3 | L4 | L5 | L6 | L7 |
|---|---|---|---|---|---|---|---|
| Calculated | 2.76 | 2.5 | 2.09 | 1.05 | 2.18 | 0.53 | 0.06 |
| Parameters | L8 | L9 | L10 | C1 | C2 | C3 | C4 |
| Calculated | 1.13 | 0.59 | 1.35 | 0.145 | 0.08 | 0.11 | 0.12 |
| Parameters | C5 | C6 | C7 | C8 | C9 | C10 | |
| Calculated | 0.08 | 0.22 | 0.24 | 0.11 | 0.0.07 | 0.04 | |

where "B" and "C" parameters are defined in (14) , (15) and "r = 50Ω":

$$B = \frac{(1 + C_3L_3S^2 + C_4L_3S^2 + C_4L_4S^2 + C_3C_4L_3L_4S^4)}{(C_2S + 2C_3S) + 2C_4S + C_2C_3L_3S^3 + C_2C_4L_3S^3 + C_2C_4L_4S^3 + 2C_3C_4L_4S^3 + C_2C_3C_4L_3S^5} \tag{14}$$

$$C = \frac{B + L_2S}{(1 + BC_1S + C_1L_2S^2)} \tag{15}$$

where "D", "E", and "F" parameters are defined in (16), (17), and (18):

$$D = \frac{(1 + C_6L_5S^2 + C_7L_5S^2 + C_7L_6S^2 + C_6C_7L_5L_6S^4)}{(C_5S + C_6S + C_7S + C_5C_6L_5S^3 + C_5C_7L_5S^3 + C_5C_7L_6S^3 + C_6C_7L_6S^3 + C_5C_6C_7L_5L_6S^5} \tag{16}$$

$$E = \frac{(1 + C_8L_8S^2 + C_9L_8S^2 + C_9L_9S^2 + C_8C_9L_5L_8L_9S^4)}{(C_8S + C_9S + C_{10}S + C_8C_{10}L_8S^3 + C_9C_{10}L_8S^3 + C_9C_{10}L_9S^3 + C_8C_9L_9S^3 + C_8C_9C_{10}L_8L_9S^5} \tag{17}$$

$$F = \frac{(D \times E)}{(D + E)} \tag{18}$$

## 4. Proposed power divider design

Figure 5 illustrates the topology of the designed Wilkinson PD. Two main resonator cells are used instead of the two long $\lambda/4$ transmission lines in the conventional PD. Therefore, the circuit size is extremely reduced and the harmonic suppression are achieved. The dimensions of the designed Wilkinson PD are as follows: d12 = 2.44, d13 = 3.50, d14 = 5.70, W9 = 1.1, W10 = 1.1, W11 = 1.1, W12 = 0.2, S8 = 0.3, S9 = 0.9, S10 = 0.2 (all in millimeter).

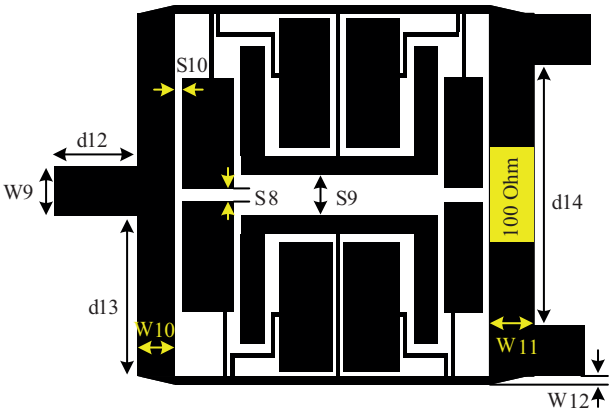


**Figure 5**. Topology of proposed Wilkinson PD.

## 5. Simulation and experimental results

The RT/Duorid 5880 substrate, with a relative dielectric constant equal to 2.2 and 31 mil thickness is considered for the simulation and implementation of the proposed PD. Figure 6 shows the implemented PD photograph with occupied size of 0.137 $\lambda_g$ × 0.076 $\lambda_g$, where $\lambda_g$ is calculated at 2 GHz.

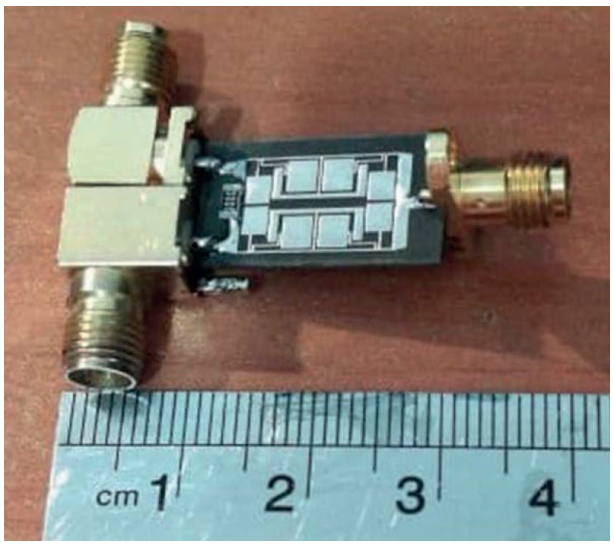


**Figure 6**. Photograph of the proposed PD.

The simulated and measured results are obtained by electromagnetic simulator advanced design system (ADS) software and an Agilent network analyzer N5230A, respectively. The simulation results of the proposed

WPD are shown in Figure 7. The comparison between the simulation and measurement results of the proposed WPD are shown in Figure 8. The measurement responses are in good agreement with the simulation results. The fabricated PD can suppress the 2nd to 14th spurious harmonics by 20, 18, 13, 26, 15, 21, 26, 18, 16, 19, 13, 17, and 16 (all in dB) respectively. The proposed PD has a fractional bandwidth of about 40%, which is calculated based on [22–25].

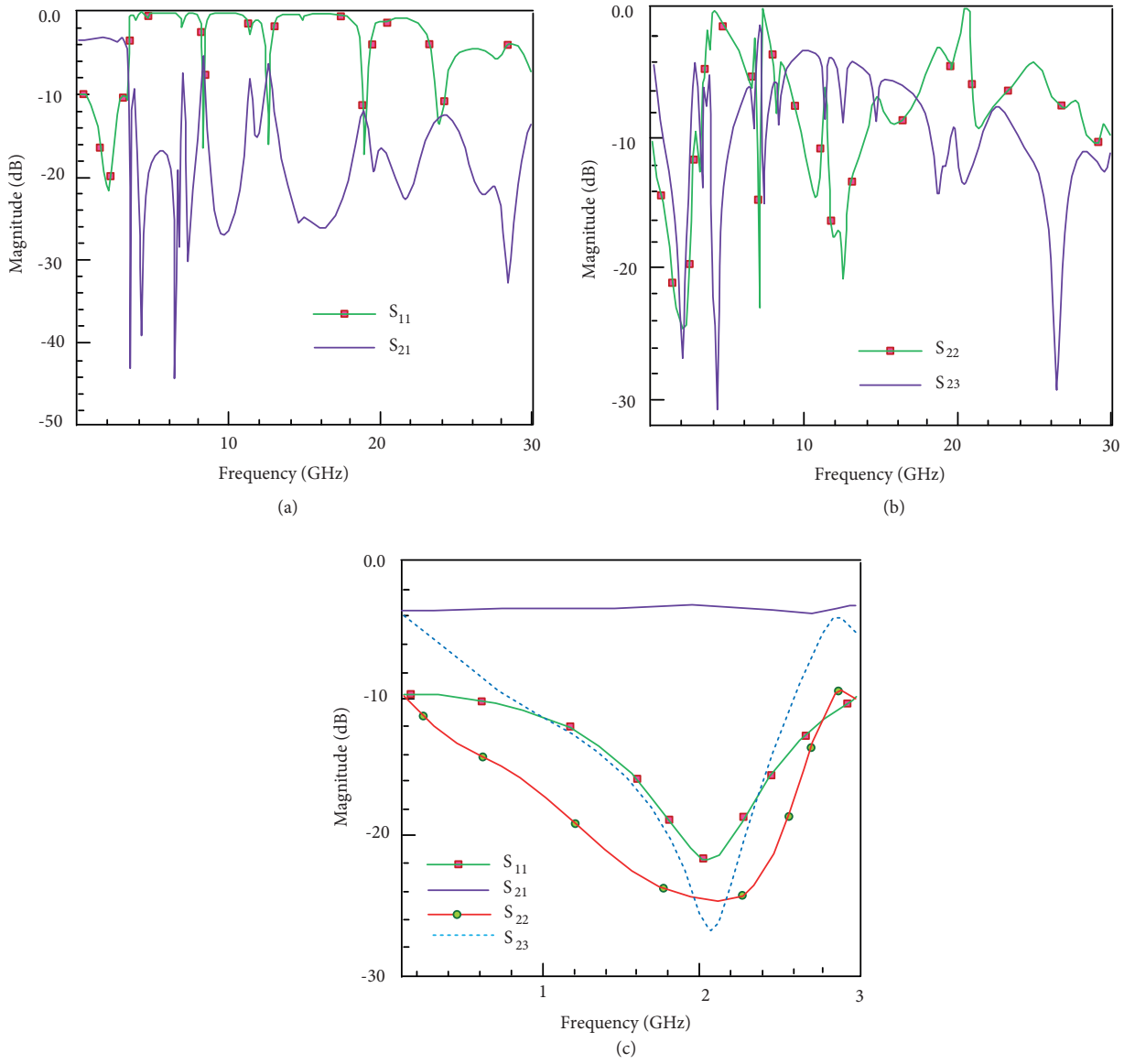


**Figure 7**. Measurement and simulation results of scattering parameters (a) S11 and S21 (b) S22 and S32 (c) in-band frequency response.

The proposed WPD is compared with related studies in Table 3. According to this table, the proposed WPD shows good performances in terms of size reduction, harmonic suppression, and fractional bandwidth parameters. Also, higher order of harmonic suppression (up to 14) is achieved in the proposed divider compared to the listed dividers in Table 3. Moreover, in terms of size reduction and fractional bandwidth (FBW), the proposed divider has an acceptable performance.

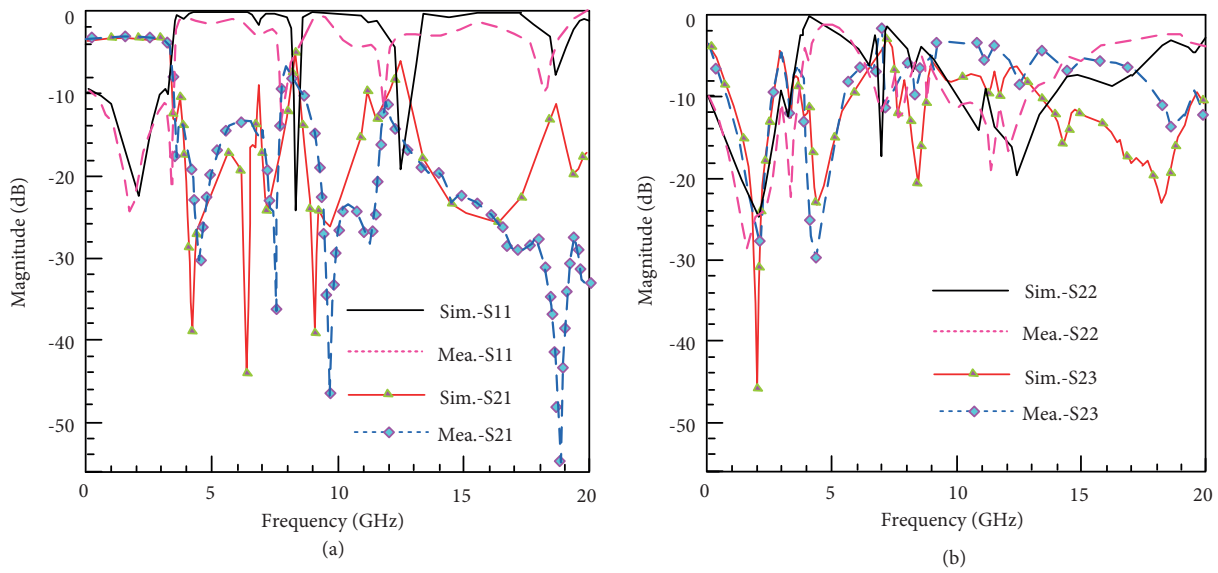


**Figure 8**. Measured and simulated scattering parameters of proposed WPD (a) S11 and S21 (b) S22 and S23.

**Table 3**. Comparison between the proposed Wilkinson PD design and other published studies.

| Ref. | FBW (%) | Relative area (%) | Harmonic suppression (dB) | | | | | | | | | | | | |
|---|---|---|---|---|---|---|---|---|---|---|---|---|---|---|---|
| | | | 2nd | 3rd | 4th | 5th | 6th | 7th | 8th | 9th | 10th | 11th | 12th | 13th | 14th |
| Conv. | 30 | 100 | - | - | - | - | - | - | - | - | - | - | - | - | - |
| [5] | - | 61 | 26 | 25 | - | - | - | - | - | - | - | - | - | - | - |
| [6] | - | 34 | 13 | 35 | - | - | - | - | - | - | - | - | - | - | - |
| [7] | - | 70.7 | - | 53 | 25 | 26 | 20 | - | - | - | - | - | - | - | - |
| [8] | 37.7 | 22.7 | 17 | 28 | 47 | 57 | 35 | 20 | - | - | - | - | - | - | - |
| [15] | - | 50 | 32 | 28 | - | - | - | - | - | - | - | - | - | - | - |
| [19] | 44 | 43.5 | 21 | 20 | 23 | 24 | 32 | - | - | - | - | - | - | - | - |
| This work | 40 | 50 | 20 | 18 | 13 | 26 | 15 | 21 | 26 | 18 | 16 | 19 | 13 | 17 | 16 |

## 6. Conclusion

A Wilkinson PD with compact size and harmonic rejection using resonator cells instead of 70.7 Ω transmission lines in the conventional circuit is designed. To verify the design procedures, the proposed PD with 50% size reduction and 13 harmonic suppression (2nd to 14th) has been fabricated. With the overall good features such as: compact size, high ability to harmonic suppression and acceptable isolation between output ports, the proposed PD is a good choice to operate in compact modern wireless circuits.

## References

[1] Wilkinson EJ. An N-way hybrid power divider. IRE Transactions on Microwave Theory and Techniques 1960; 8 (1): 116-118. doi: 10.1109/TMTT.1960.1124668.

[2] Pozar DM. Microwave Engineering. USA: John Wiley and Sons, 2009.

[3] Zhu L, Sun S, Li R. Microwave Bandpass Filters For Wideband Communications. USA: John Wiley and Sons, 2011.

[4] Li J, Liu Y, Li S, Yu C, Wu Y. Miniaturisation of microstrip planar Bagley polygon power divider with dual transmission lines. Electronics Letters 2013; 49 (16): 1015-1016. doi: 10.1049/el.2013.1524

[5] Zhang F, Li CF. Power divider with microstrip electromagnetic bandgap element for miniaturisation and harmonic rejection. Electronics Letters 2008; 44 (6): 422-424. doi: 10.1049/el:20083693

[6] Yang J, Gu C, Wu W. Design of novel compact coupled microstrip power divider with harmonic suppression. IEEE Microwave and Wireless Components Letters 2008; 18 (9): 572-574. doi: 10.1109/LMWC.2008.2002444

[7] Hayati M, Roshani S, Roshani S. Miniaturized Wilkinson power divider with nth harmonic suppression using front coupled tapered CMRC. Applied Computational Electromagnetics Society (ACES) Journal 2013; 28 (3): 221-227. doi: 10.1007/s10470-018-1299-x

[8] Siahkamari H, Makki SV, Malakooti SA. Using microstrip LPF in Gysel power divider for extreme size reduction and higher order harmonic suppression. Frequenz 2015; 69 (7-8): 323-328. doi: 10.1515/freq-2014-0213.

[9] ] Roshani S, Siahkamari P, Siahkamari H. Compact harmonic suppressed Gysel power divider with plain structure. Frequenz 2017; 71 (5-6): 221-226. doi: 10.1515/freq-2016-0024

[10] Li M, Wu Y, Qu M, Li Q, Liu Y. A novel power divider with ultra-wideband harmonics suppression based on double-sided parallel spoof surface plasmon polaritons transmission line. International Journal of RF and Microwave Computer-Aided Engineering 2018; 28 (4): 1-7. doi: 10.1002/mmce.21231.

[11] Roshani S. A Wilkinson power divider with harmonics suppression and size reduction using meandered compact microstrip resonating cells. Frequenz 2017; 71 (11-12): 517-522. doi: 10.1515/freq-2016-0149

[12] Moradi E, Moznebi AR, Afrooz K, Movahhedi M. Gysel power divider with efficient second and third harmonicmsuppression using one resistor. AEU-International Journal of Electronics and Communications 2018; 89 (7): 116-122. doi: 10.1016/j.aeue.2018.03.011

[13] Wang X, Shinoda N, Ma Z, Ohira M. Tunable transmission-line transformer with two varactors and its application for Wilkinson power divider. AEU-International Journal of Electronics and Communications 2019; 98 (1): 259-264. doi: 10.1016/j.aeue.2018.11.017

[14] ]Rostami P, Roshani S. A miniaturized dual band Wilkinson power divider using capacitor loaded transmission lines. AEU-International Journal of Electronics and Communications 2018; 90 (8): 63-68. doi: 10.1016/j.aeue.2018.04.014

[15] Chen FJ, Wu LS, Qiu LF, Mao JF. A four-way microstrip filtering power divider with frequency-dependent couplings. IEEE Transactions on Microwave Theory and Techniques 2015; 63 (10): 3494-3504. doi: 10.1109/TMTT.2015.2457426

[16] Yang X, Zhang X, Liao Z. A novel planar four-way Power divider with large dividing ratio. AEU-International Journal of Electronics and Communications 2018; 85 (3): 1-6. doi: 10.1016/j.aeue.2017.12.028

[17] Guo Z, Yang T. A novel compact Wilkinson power divider with controllable harmonic suppression and simple structure. Journal of Electromagnetic Waves and Applications 2018; 32 (5): 601-608. doi: 10.1080/09205071.2017.1400926

[18] Kumar M, Islam SN, Sen G, Parui SK, Das S. Design of compact Wilkinson power divider with harmonic suppression for GSM application. In: IEEE Applied Electromagnetics Conference (AEMC); Aurangabad, India; 2017. pp. 1-2. doi: 10.1109/AEMC.2017.8325635

[19] Karimi G, Menbari S. A novel Wilkinson power divider using lowpass filter with harmonics suppression and high fractional bandwidth. Microelectronics Journal 2018; 71 (1): 61-69. doi: 10.1016/j.mejo.2017.11.011

[20] Heydari M, Roshani S. Miniaturised unequal Wilkinson power divider using lumped component elements. Electronics Letters 2017; 53 (16): 1117-1119. doi: 10.1049/el.2017.2118

[21] Song K, Hu S, Zhang F, Zhu Y, Fan Y. Compact dual-band filtering-response power divider with high in-band frequency selectivity. Microelectronics Journal 2017; 69 (11): 73-76. doi: 10.1016/j.mejo.2016.03.002

[22] Jamshidi M, Lalbakhsh A, Lotfi S, Siahkamari H, Mohamadzade B et al. A neuro-based approach to designing a Wilkinson power divider. International Journal of RF Microwave Computer Aided Engineering 2019; 1: 1-20. doi: 10.1002/mmce.22091

[23] Lotfi S, Hayati M. Compact low-pass filter with ultra-wide stopband using analysed triangular-shaped resonator. Electronics Letters 2017; 53 (15): 1050-1052. doi: 10.1049/el.2017.1169

[24] Karimi G, Lotfi S, Siahkamari H. Design of microstrip Lowpass filter with sharp roll-off using elliptical and radial resonators. Frequenz 2017; 71(7-8): 349-356. doi: 10.1515/freq-2016-0111

[25] Jamshidi M, Siahkamari H, Roshani S, Roshani S. A compact Gysel power divider design using U-shaped and T-shaped resonators with harmonics suppression. Electromagnetics 2019; 39 (7): 491-504. doi: 10.1080/02726343.2019.1658165

[26] Hayati M, Abdipour A, Abdipour A. A Wilkinson power divider with harmonic suppression and size reduction using high-low impedance resonator cells. Radioengineering 2015; 24(1):137-41. doi: 10.13164/re.2015.0137

[27] Lotfi S, Roshani S, Roshani S, Gilan MS. Wilkinson Power Divider with Band-pass filtering response and harmonics suppression using open and short stubs. Frequenz 2020; 74(5-6): 169-176. doi: 10.1515/freq-2019-0200